archives
of thermodynamics
Vol. **40**(2019), No. 1, 21–48
DOI: 10.24425/ather.2019.128288

Relation between thermal conductivity and coordination number for fibre-reinforced composite with random distribution of fibres

PIOTR DARNOWSKI*
PIOTR FURMAŃSKI
ROMAN DOMAŃSKI

Institute of Heat Engineering, Warsaw University of Technology,
Nowowiejska 21/25, 00-665 Warszawa, Poland

Abstract Transverse effective thermal conductivity of the random unidirectional fibre-reinforced composite was studied. The geometry was circular with random patterns formed using random sequential addition method. Composite geometries for different volume fraction and fibre radii were generated and their effective thermal conductivities (ETC) were calculated. Influence of fibre-matrix conductivity ratio on composite ETC was investigated for high and low values. Patterns were described by a set of coordination numbers (CN) and correlations between ETC and CN were constructed. The correlations were compared with available formulae presented in literature. Additionally, symmetry of the conductivity tensor for the studied geometries of fibres was analysed.

Keywords: Fibre reinforced composite; Random sequential addition; Parallel fibres; Coordination number; Effective thermal conductivity

Nomenclature

a	–	fibre radius, m
A	–	area, m^2
a/R	–	ratio of fibre radius to matrix radius
c_p	–	specific heat capacity, J/(kg K)
CN	–	coordination number

*Corresponding Author. Email: piotr.darnowski@itc.pw.edu.pl

d	–	number of dimensions or fibre diameter
ETC	–	effective thermal conductivity, W/(m K)
f	–	volume fraction
f_0	–	matrix volume fraction
f_1	–	fibre volume fraction
$\mathbf{I}$	–	unit tensor
$\mathbf{K}$	–	thermal conductivity tensor
k_1	–	fibre thermal conductivity, W/(m K)
k_0	–	matrix thermal conductivity, W/(m K)
k_{eff}	–	effective thermal conductivity (ETC), W/(m K)
k_{ij}	–	thermal conductivity tensor components $i, j = x, y, z$ in any frame of reference and $i, j = 1, 2, 3$ in principal frame of reference, W/(m K)
L	–	composite length, m
N	–	number of particles/fibres
n	–	number of element
$\vec{n}$	–	normal vector
$\vec{q}$	–	heat flux vector
q_n	–	normal heat flux $q_n = \vec{q} \cdot \vec{n}$, W/(m^2 K)
r	–	radius, m
R	–	composite radius, m
RMSE	–	root mean squared error
RSD	–	relative standard deviation
T	–	temperature, K
V	–	volume, m^3
Z	–	coordination number (CN)
Z_2	–	CN calculated for constant neighbourhood regions radius
Z_4	–	CN calculated for neighbourhood radius equal pair distribution functions' function first minima
$< \cdot >$	–	volume averaging
$(\dot{\cdot})$ or $\tilde{\cdot}$	–	modified parameter

Greek symbols

β	–	Bergman's contrast parameter
ζ_2	–	three-point parameter
$\mathbf{\Lambda}$	–	conductivity tensor in principal frame of reference
ρ	–	density, kg/m^3
σ	–	standard deviation (SD)

1 Introduction

Composite materials are the backbone of modern engineering. Those materials create plenty of opportunities in many engineering fields by enhancing mechanical, electromagnetic and thermal properties of construction materials. From design of light boats to construction of very complicated space crafts, new composites have growing importance in the whole engineering design.

Detailed mathematical description of complex composites involves sophisticated formalism like random geometry. A remarkable reference in the field of random materials is the monograph by Torquato which guides all relevant research before 2002 and introduces the general theory [1]. Nevertheless, plenty of new research has been published until now.

This paper focuses on description of transport (electric or thermal) properties of composites reinforced by highly conductive fibres. These properties depend on such fundamental parameters as composite composition, properties of the constituents and their distribution in the matrix. The way of distribution of constituents for the two-constituent media and in the case when one of the constituents is dispersed in the other constituent – matrix may be described in a simplified way by the quantity called a coordination number. In general, the coordination number (CN) is an average number of neighbourhoods of an object (particle, atom, fibre, etc.) but there is no one strict definition of this quantity – it depends on the field of interest. For example, in the case of regular three-dimensional cubic array of atoms (abbreviated as cP) coordination number equals to six – every atom has bounds with six other atoms. Differently in granular media, for two-dimensional circular cylinders packing in hexagonal lattice, which is most dense packing, coordination number equals six. Coordination number for any other packing structure in two dimensions, random or regular is bounded by this value [2].

Certain amount of correlations between coordination number and properties like thermal conductivity are available in the literature. Unfortunately, all the research revised pertains to three dimensional systems as they are more practical and applicable in engineering [3]. Recently with development of nanoscience two-dimensional systems become more important and applicable.

Most of the research employing CN to random heterogeneous materials treats about granular media, pebble beds or powders because this number has significant role in description of their structure [3], however it is rarely used to describe the composite structures [4]. Moreover, no correlations between the effective thermal conductivity (ETC) and CN for two dimensional systems and in particular for the random sequential addition (RSA) packing scheme seem to exist in literature, where the RSA scheme is process of random adding of fibres one by one into matrix without intersecting others and composite boundaries [5]. Traditional attempt to CN as the mean number of direct contacts does not fulfil its role for the RSA and that is

why both modified sequential analysis (SA) and pair distribution function (PDF) integration were further used [2,6]. The coordination number computed by the SA method is a simple sum of CNs for every object in the population divided by population magnitude [7]. Otherwise, CN calculated by integration of the pair distribution function is more general approach based on statistical mechanics where PDF function describes probability distribution of distances between two particles in an ensemble of particles [8,9].

The main purpose of this research is to find a correlation between the coordination number and effective thermal conductivity, taking into account size of the particles. It seems quite intuitive that the volume fraction of fibres and the ratio of the conductivities of fibre to matrix (k_1/k_0) affects mean properties of a composite material as was earlier observed [1,10]. However, it is also well known that this property depends on the geometrical arrangement of constituents. Therefore, we intend to verify if it is possible to predict effective conductivity knowing only coordination number. Moreover, it is expected that the size of the fibres has an impact on the correlation and it should be analysed.

The additional goal was to investigate quantitatively the symmetry of the conductivity tensor in random composites. If this tensor is symmetric it can be awaited that the analysed composite is isotropic on the macroscopic level. A random distribution of fibres can lead to anisotropy in the properties especially in case of finite composite where size of particle is non-negligible. It seems therefore to be important issue because most correlations between ETC and volume fraction assume that the medium is isotropic.

2 Correlations for the effective thermal conductivity presented in literature

Not many formulae for the effective thermal conductivity of two-component media containing randomly located fibres have been presented in literature. They were used for comparison with numerical results further in the present paper.

Historically the first and simplest correlation was derived theoretically by Clausius-Mossotti for small volume fractions [11–13]:

$$\frac{k_{eff}}{k_0} = \frac{1 + f\beta}{1 - f\beta}\,, \tag{1}$$

where Bergman's contrast parameter β for k_1 fibre and k_0 matrix conductivities respectively, is defined as

$$\beta = \frac{k_1 - k_0}{k_0 + k_1} \,. \tag{2}$$

This formula is valid for statistically isotropic random media with no interaction between fibres taken into account.

Torquato presented another formula based on an expansion in series versus contrast for two-phase isotropic and disordered media with impenetrable cylinders or spheres [1,13]:

$$\frac{k_{eff}}{k_0} = \frac{1 + (d-1)f_1\beta - (d-1)f_0\zeta_2\beta^2}{1 - f_1\beta - (d-1)f_0\zeta_2\beta^2} \,, \tag{3}$$

where d is a number of space dimensions, f_0 is the volume fraction of the matrix and $f = f_1 = 1 - f_0$ is the volume fraction of the dispersed phase. Three-point parameter ζ_2 is here responsible for microstructure. It was derived by Torquato and Lado [14] for isotropic equilibrium distribution of identical hard cylinders in a matrix and given as

$$\zeta_2 = \frac{f}{3} - 0.05707 f^2 \,. \tag{4}$$

Equation (1) can be derived from Eq. (3) by setting $\zeta_2 = 0$ and $d = 2$.

Czapla *et al.* [11] obtained a formula for the ETC in the form of power series

$$\begin{aligned} \frac{k_{eff}}{k_0} = {} & 1 + 2f\beta + 2f^2\beta^2 + 4.9843 f^3\beta^3 - 6.829 f^4\beta^3 \\ & + 4.2139 f^5\beta^3 - 0.3462 f^6\beta^3 - 0.0688 f^3\beta^4 + 7.3652 f^4\beta^4 \\ & - 12.4218 f^5\beta^4 + 7.0868 f^6\beta^4 - 0.1463 f^3\beta^5 \\ & + 6.3079 f^4\beta^5 - 10.4599 f^5\beta^5 + 6.7108 f^6\beta^5 \\ & - 0.7996 f^3\beta^6 + 4.517 f^4\beta^6 - 7.8602 f^5\beta^6 + 5.9897 f^6\beta^6 \,. \end{aligned} \tag{5}$$

It was derived for unidirectional infinite circular cylinders randomly distributed in a uniform matrix and is claimed to be valid for any concentration [11]. In order to carry out more general comparison additionally two approximate formulae for the effective thermal conductivity of composites with periodic arrays of inclusions were considered, which were derived by Perrins, McKenzie, and McPherdan [1,15,16], for square lattice:

$$\frac{k_{eff}}{k_0} = 1 + \frac{2\beta f}{1 - \beta f - 0.305827\beta^2 f^4} \tag{6}$$

and for hexagonal lattice:

$$\frac{k_{eff}}{k_0} = 1 + \frac{2\beta f}{1 - \beta f - 0.075422\beta^2 f^6} \,. \tag{7}$$

They are assumed to be valid for a relatively low volume fractions of fibres.

3 Composite geometry and way of determination of the effective thermal conductivity

Heat conduction in the transverse direction (Y-direction – XY-plane) for infinitely long cylinder composite with cylindrical fibres parallel to Z-axis was analysed, see Fig.1.

Most of the theoretical research treats composite systems as infinite. As it is impossible to simulate numerically the infinite media, the simulation techniques are typically applied to a square or circle domain (cube or sphere in 3D) [1,17]. In case of circular system, there is usually one central ('reference') particle assumed and, for example, the pair-distribution function is computed for this particle by generation of many (thousands) of different distributions of neighbouring particles (geometry realizations), which are subsequently ensemble averaged. This approach does not give opportunity to analyse finite random system properties due to preferred location of the central particle. In the case of square geometry typically periodic boundary conditions (BC) are applied to simulate infinite structures. But, the periodicity creates recurrent pattern and it is not obvious that it ensures proper randomness and isotropy. On the contrary system investigated in this paper is the finite one in order to analyse the related effects. The external boundary is circular because authors' anticipate that, it is more natural to investigate anisotropy and it has highest inherent level of symmetry.

Fibres were packed by the random sequential addition (RSA) scheme [5]. They are added one by one with restrictions that they cannot intersect with each other and the external boundary. Sample geometry of composite is shown in Fig. 1.

One hundred twenty such random patterns were created. Three volume fractions were chosen and analysed $f = 0.3,\ 0.4$, and 0.49 with four different radii of particles assumed, i.e., $a/R = 0.04,\ 0.06,\ 0.08$, and 0.1, where R is the matrix radius. Different geometries were created for every particular radius and corresponding volume fraction. The highest volume fraction,

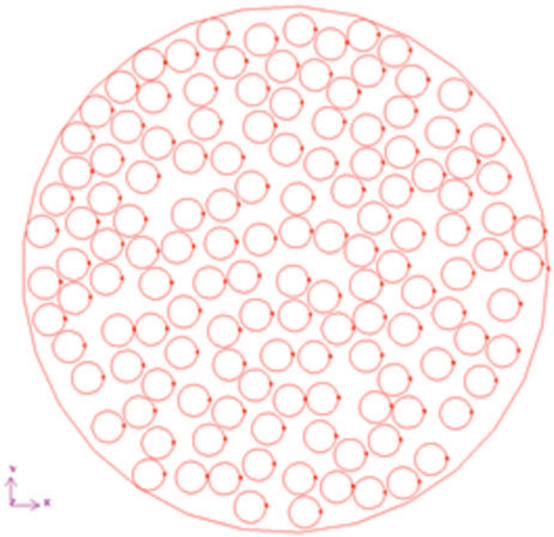

Figure 1: Example geometry of composite with $f = 0.49$ and $N = 136$ particles and fibres with radius $a = 0.6R$.

$f = 0.49$, was chosen as its value is relatively close to saturation limit [5] for the RSA method (corresponding to ~ 0.55) and due to difficulty in obtaining higher f in reasonable computational time. Particles radii were selected arbitrary from relatively large ($a/R = 0.1$) to relatively small ($a/R = 0.04$), where R is the matrix radius.

The effective thermal conductivity (ETC) for random heterogeneous media is defined in a way similar to the classical Fourier law used in heat conduction [1,18,19]

$$\langle \vec{q} \rangle = -\mathbf{K} \cdot \langle \nabla T \rangle \ , \tag{8}$$

where $\langle \vec{q} \rangle$ is the mean heat flux vector, $\langle \nabla T \rangle$ denotes the mean temperature gradient, $\mathbf{K}$ is the second order effective thermal conductivity tensor while $\langle \rangle$ denotes the volume averaging procedure. Detailed derivation of ETC relations is presented in Appendix A. Assuming that temperature gradient occurs only in Y-direction, the formulae for the non-zero $\mathbf{K}$ components are:

$$k_{yy} = \frac{-\oint_A y(\vec{q} \cdot \vec{n}) dA}{\left\langle \frac{\partial T}{\partial y} \right\rangle V} \ , \tag{9}$$

$$k_{xy} = \frac{-\oint_A x(\vec{q} \cdot \vec{n}) dA}{\left\langle \frac{\partial T}{\partial y} \right\rangle V} \ , \tag{10}$$

where the volume of composite is $V = \pi L R^2$ and its length was set as $L = 1.0$ in arbitrary units. Scalar $q_n = \vec{q} \cdot \vec{n}$ stands for the heat flux on the outer surface of the elementary surface element of composite. The mean heat flux was calculated using the simplified numerical formulae:

$$\langle q_y \rangle = \frac{1}{V} \sum_{i=1}^{n} q_n \, y \Delta A \, , \tag{11}$$

$$\langle q_x \rangle = \frac{1}{V} \sum_{i=1}^{n} q_n \, x \Delta A \, , \tag{12}$$

where $\Delta A = A/n$ is a ratio of the total external surface area $A = 2\pi RL$ to the n – number of elements on this surface.

The steady state of heat conduction without heat sources with fixed thermal conductivity of each phase and no contact resistance at the fibre-matrix interface were assumed in the composite. In order to find the ETC it was necessary to determine at first the temperature distribution in the composite solving the Laplace equation and accounting for continuity of temperature and heat fluxes at the fibre-matrix interfaces [18]:

$$\nabla^2 T_i = 0 \, , \tag{13}$$

where $i = 0$ for matrix and $i = 1$ for fibre. The first boundary condition (BC) on the border between fibre and matrix states that there should be the same temperature, $T_{0,int} = T_{1,int}$, and the second boundary condition demands continuity of heat fluxes on the interfaces, $(k_0 \partial T/\partial n)_{0,int} = (k_1 \partial T/\partial n)_{1,int}$. The external boundary conditions are formulated in such a way as to obtain the constant temperature gradient in one direction (Y or X). This allows to perform simpler computation of the ETC – see Appendix A. Therefore, for the outer cylindrical region (Fig.1) temperature distribution obeying the following formula was adopted:

$$T = T_R + c \, \langle \nabla T \rangle \cdot \vec{n} \, , \tag{14}$$

where c is a constant and T_R is the reference temperature and $\vec{n}$ is vector normal to the surface. For the circular boundary of the composite the normal vector has the same direction as the vector locating a point on the composite outer surface with the origin in the circle centre: $\vec{n} = \vec{r}/|\vec{r}|$. To satisfy the condition that $\langle \nabla T \rangle$ is the mean temperature gradient in the composite the constant c should be equal to matrix radius $\vec{r} = R$, i.e.,

$$T = T_R + \langle \nabla T \rangle \cdot \vec{r} \, . \tag{15}$$

4 Correlating the effective thermal conductivity with the coordination number

The coordination number (CN) is one of the fundamental parameter describing the geometry in heterogeneous media of any type. In most cases it is understood as number of direct contact with given particle (atom, molecule, fibre, etc.). Unfortunately, the RSA packing method of particles is based on statistical 'parked' [1] process and probability of direct contact of sampled particles tends to zero [8]. In such case it is not feasible to calculate useful coordination number by counting direct contact of particles [6,8]. To solve this problem a notion of the neighbourhood area was introduced. A particle becomes the neighbour when it crosses area of the neighbourhood.

Two forms of this idea were utilized. The first one was the constant neighbourhood circular region around every particle with radius equal $r/d = 1.5$ [2,9] with the corresponding coordination number denoted as Z_4. The second form assumes that the neighbourhood region radius is equal to the location of the first minimum of the pair distribution function (X_0) and it was marked by the symbol Z_2 [8].

In order to calculate CN, two methods were identified to combine with the neighbourhood regions described above. The first method was based on integration of the pair distribution function from zero to the radius of neighbourhood area [5]. The second method used the sequential analysis (SA), which is based on simple counting process of particles and calculating mean numbers of particles in vicinity of the given particle [7].

Detailed description of the methods and their modifications used to evaluate CN, were described in paper [6]. It was shown there that the coordination number calculated from integration of the pair distribution function and the sequential analysis are equivalent for the same neighbourhood radius. Therefore, only the SA method was used in the present paper. Following Eq. (3) the general relationship for the ETC was assumed in the form

$$\frac{k_{eff}}{k_0} = \phi\left(\mathrm{f},\beta,\zeta_2\right) \ , \tag{16}$$

where ϕ is the function symbol. Equation (4) defines ζ_2 for isotropic random distribution of the unidirectional fibres in an infinite medium and this parameter is function of volume fraction only.

It was shown that volume fraction could be connected with the coordi-

nation number (CN) for the RSA packing by approximate relation [2]

$$Z_4(f) = 6.8898 f^2 + 4.3608 f \ . \tag{17}$$

This equation shows that average Z_4 and f are quantities related explicitly. It is known that CN (Z_4) is responsible for microstructure of the system similarly as f and ζ_2 and it is possible that those quantities are coupled. Nevertheless, it is not obvious if such coupling exists in any conditions.
An attempt to find out what influence the CN exerts on the ETC in the finite system and therefore to figure out what conditions should be met to consider the system to be infinite were analysed in this paper. Development of the respective correlations was difficult and required some compromises. First of all, it was assumed that the general form of expression for the ETC, corresponding to Eq. (3), is valid because it reduces to Clausius-Mossotti relation (Eq. (1)) for small volume fractions. Hence, only the three-point parameter ζ_2 was modified. Secondly the CN (Z_4) was used as microstructure parameter and introduced into modified ζ_2. Moreover a/R was added to the new relation for ζ_2 to introduce finite size effects on the ETC of the composite. Moreover, it was expected that new expression for the ETC becomes equivalent to Eq. (3) when system size becomes infinite relative to fibre dimension ($a/R \ \to 0$). The modified three-point parameter $\overline{\zeta_2}$ was sought in form

$$\overline{\zeta_2} = \Phi\left(\frac{\mathrm{a}}{\mathrm{R}}, \mathrm{Z}_4, \beta\right) \ , \tag{18}$$

where Φ is the function symbol. It should be noted that in the proposed correlation not only a/R and Z_4 instead of f were used but also the parameter β was introduced as it was noticed that it had some effect on the results.

5 Symmetry of the effective thermal conductivity tensor

The system analysed in this work, due to unidirectional fibre alignment, has monoclinic symmetry [1]. Therefore, anisotropy of the ETC can be expected only in XY-plane – Fig. 1. Hence the effective thermal conductivity tensor can be expressed as

$$\mathbf{K} = \begin{bmatrix} k_{xx} & k_{xy} & 0 \\ k_{yx} & k_{yy} & 0 \\ 0 & 0 & k_{zz} \end{bmatrix} \ . \tag{19}$$

If additionally, $k_{yy}= k_{xx}$, the composite becomes transversely isotropic [1]. In the ideal case of radially infinite (in XY plane) system with a random distribution of unidirectional fibres it should be transversely isotropic. Simulations were performed to investigate if the analysed composites with relatively large fibres distributed in the matrix according to the RSA could be described in terms of simpler symmetry as transversely isotropic [1].

In physical systems, thermal conductivity tensor must be symmetric so non-diagonal components should obey the condition $k_{ij} = k_{ji}$, where $i, j = x, y, z$ [1,20]. Additionally, due to the 2nd law of thermodynamics, the matrix formed from tensor components should be positive definite so all of its eigenvalues should be positive [1]. For simulations presented here possibility of occurrence of nonphysical rotational heat flux as an effect of numerical or methodology errors have been taken into account.

Generally, tensor $\mathbf{K}$ can be decomposed into the symmetric (k^s_{ij}) and anti-symmetric (k^a_{ij}) parts by transformations [20]

$$\begin{cases} k^s_{ij} = \frac{k_{ij}+k_{ji}}{2} , \\ k^a_{ij} = \frac{k_{ij}-k_{ji}}{2} , \end{cases} \tag{20}$$

and after such transformation ($\mathbf{K} = \mathbf{K}^{\mathrm{a}} + \mathbf{K}^{\mathrm{s}}$)

$$\begin{bmatrix} k_{xx} & k_{xy} & 0 \\ k_{yx} & k_{yy} & 0 \\ 0 & 0 & k_{zz} \end{bmatrix} = \begin{bmatrix} k^s_{xx} & k^s_{xy} & 0 \\ k^s_{xy} & k^s_{yy} & 0 \\ 0 & 0 & k^s_{zz} \end{bmatrix} + \begin{bmatrix} 0 & k^a_{xy} & 0 \\ -k^a_{xy} & 0 & 0 \\ 0 & 0 & 0 \end{bmatrix} . \tag{21}$$

The symmetric part $\mathbf{K}^{\mathrm{s}}$ can be diagonalized by tensor $\mathbf{P}$ and therefore after multiplication both sides of Eq. (19) by this tensor sides the following decomposition is obtained:

$$\mathbf{\Lambda} = \mathbf{P}^{-1}\mathbf{K}\mathbf{P} = \mathbf{P}^{-1}\left(\mathbf{K}^{\mathrm{a}}+\mathbf{K}^{\mathrm{s}}\right)\mathbf{P} = \mathbf{P}^{-1}\mathbf{K}^{\mathrm{a}}\mathbf{P} + \mathbf{P}^{-1}\mathbf{K}^{\mathrm{s}}\mathbf{P} = \mathbf{\Lambda}^{\mathrm{s}}+\mathbf{\Lambda}^{\mathrm{a}} , \tag{22}$$

where $\mathbf{P}$ is invertible matrix with eigen-vectors of $\mathbf{K}^{\mathrm{s}}$ as columns, $\mathbf{\Lambda}^{\mathrm{s}}$ is a diagonal tensor and $\mathbf{\Lambda}^{\mathrm{s}}$ is a non-diagonal tensor. The thermal conductivity tensor after diagonalization using $\mathbf{P}$ matrix was adjusted to the monoclinic symmetry and assumes the form

$$\mathbf{\Lambda} = \begin{bmatrix} k_{11} & 0 & 0 \\ 0 & k_{22} & 0 \\ 0 & 0 & k_{33} \end{bmatrix} + \begin{bmatrix} 0 & k_{12} & 0 \\ -k_{12} & 0 & 0 \\ 0 & 0 & 0 \end{bmatrix} . \tag{23}$$

The anti-symmetric component of the tensor should disappear for physical system as it leads to occurrence of the spiral heat flow, which was not observed experimentally [20].

In order to analyse the symmetry of the conductivity tensor it is required to find k_{yx} and k_{xx} components. Instead of constant temperature gradient in Y-direction ($\frac{\partial T}{\partial y}$) also gradient in X-direction is applied $\langle \nabla T \rangle = \left[\begin{array}{ccc} \left\langle \frac{\partial T}{\partial x} \right\rangle & 0 & 0 \end{array} \right]^T$ leading to new equations for the ETC components:

$$k_{xx} = \frac{-\oint_A x(\vec{q} \cdot \vec{n}) dA}{\left\langle \frac{\partial T}{\partial x} \right\rangle V} , \tag{24}$$

$$k_{yx} = \frac{-\oint_A y(\vec{q} \cdot \vec{n}) dA}{\left\langle \frac{\partial T}{\partial x} \right\rangle V} . \tag{25}$$

6 Numerical procedure an materials

Typical heat transfer simulations requiring solution of partial differential equations are conducted by finite element method (FEM), finite difference method (FDM) or finite volume method (FVM). Nevertheless, those methods have limited numerical capabilities when both many boundary conditions (BC) and complex geometry are applied. Problems with these issues especially appear in analysis of complex structures like porous or granular media. What is remarkable even for calculations performed here, for two dimensional systems such complications appeared. Plenty of recent works emphasis on using new computational methods like lattice Boltzmann method (LBM) which allows creating complicated BC without huge increase in computational time [21,22]. Nevertheless, in this work the popular and widely proven FVM code Fluent has been used [23].

Triangular unstructured mesh was used with similar mesh size for every case. Mesh grids parameters were calculated by computer code and then used in automatic generation of input file for Gambit 2.4.6 software [24]. Such mesh was satisfactory for small number of particles (Fig. 3) but quality was poorer for huge number of particles (Fig. 2).

Creation of mesh was problematic because of the appearance of very small distances between particles and between particles and boundary. The most troublesome was possibility of occurrence of direct (or almost direct) contact between particles. In such case automatic generation of mesh was

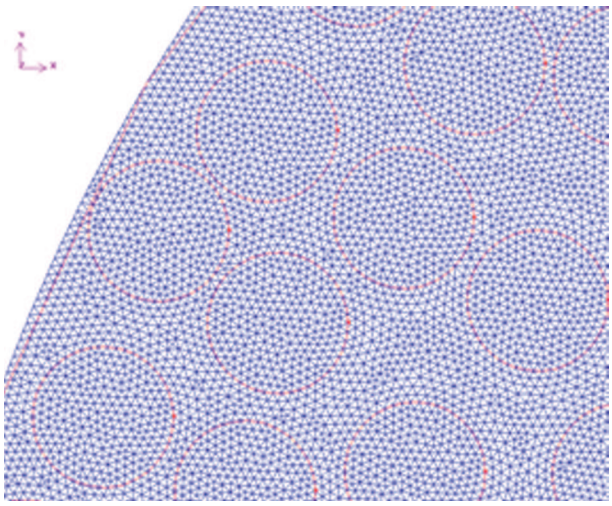

Figure 2: Part of mesh for case with the highest number of particles $N = 306$, volume fraction $f = 0.49$.

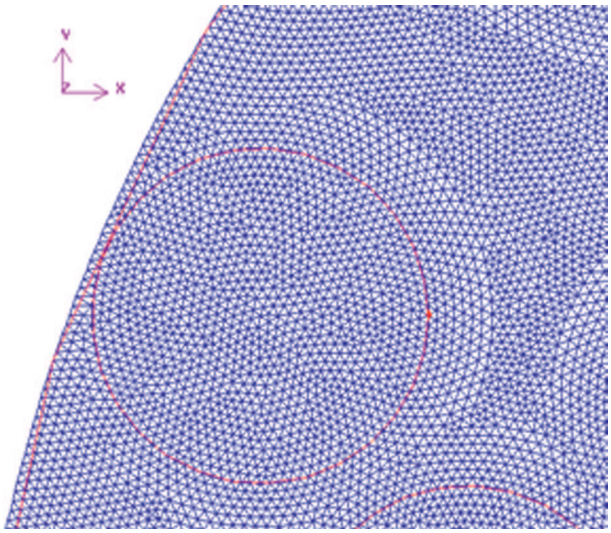

Figure 3: Part of mesh lowest number of particles $N = 30$ and $f = 0.3$.

impossible without special treatment. The problem was solved by increasing the diameter of the particles (temporary) during their sampling by about 1%. This margin gave a chance to create mesh between very close particles. The error introduced by such treatment is not significant. In ran-

dom methods like RSA probability of perfect contact tends to zero [8], so penalty on calculations of conductivity due to loss of contact effects should be much smaller than for patterns generated by other packing methods where direct contact is more common.

In spite of the undertaken actions to avoid it, the problem with mesh generation still exists (Fig. 2). In space between close particles there are not enough mesh elements to perform calculations with enough high accuracy. The example of mesh for low particle density (Fig. 3) reveals denser mesh between particles but still some particles are very close to boundary and there are few layers of mesh elements. The obvious solution would be to create finer mesh but it will demand manual mesh creation or using of more sophisticated algorithms to create the input file.

Materials making the composites were chosen arbitrary. The fibres were assumed to be from diamond with conductivity 2000 $\frac{\mathrm{W}}{\mathrm{m\,K}}$. Two types of a matrix were considered, one of copper (Cu case) with conductivity 387.6 $\frac{\mathrm{W}}{\mathrm{m\,K}}$, relatively high compared to fibres ($k_1/k_0 = 5.16$, $\beta_{\mathrm{Cu}} = 0.675322$) while the second one from magnesium (Mg case) with relatively low conductivity 7.82 $\frac{\mathrm{W}}{\mathrm{m\,K}}$ compared to fibres ($k_1/k_0 = 255.75$, $\beta_{Mg} = 0.99221$).

7 Results

For every particular case with given f, a/R, k/k_0 numerical data contained ten random geometries and altogether, 120 different geometrical patterns and 240 cases were studied. The root mean squared error (RMSE) was used as a quantitative indicator of deviation of numerical data from the proposed correlations dependent both on the fibre volume fraction and coordination number.

Numerical data for high and low conductivity ratio (Mg or Cu, (k_1/k_0)) was compared with formulae given by Torquato, Czapla, and Claussius-Mossotti (C-M) – Eqs. (3), (5), and (1), respectively. Results are presented in Fig. 4 with additional curves for regular structures Eq. (6) and (7). Moreover, Tab. 1 presents the RSME between values obtained from simulation and the mentioned formulae.

It can be observed that the RMSE (Tab. 1) for all cases increases with the fibre size and conductivity ratio. For the same particle size and different (k_1/k_0) it could be even one order of magnitude higher. For different fibre size, the RMSE can change by a factor of six.

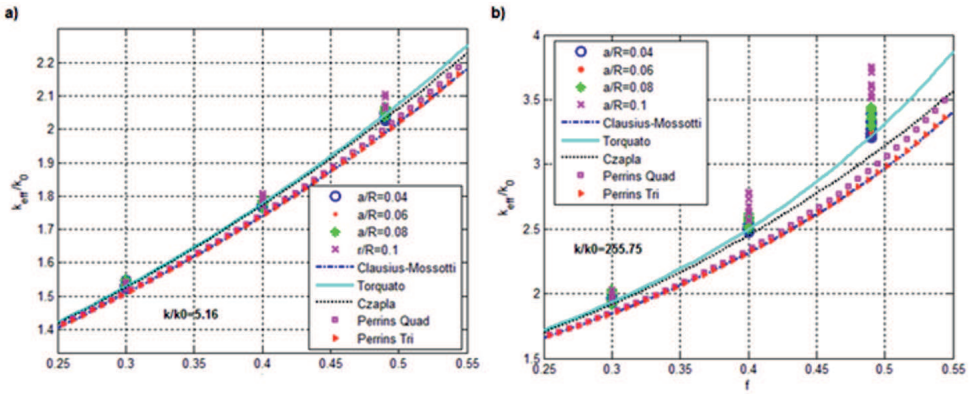

Figure 4: Effective thermal conductivity versus volume fraction. Comparison of numerical data for different particle size with analytical formulae for fibre to matrix conductivity ratio: a) $k/k_0 = 5.16$, b) $k/k_0 = 255.75$.

Table 1: Discrepancy between dimensionless ETC numerical data and values from analytical expressions (RMSE values) for different dimensionless fibre size (a/R) and fibre/matrix thermal conductivity ratio. Last row presents RMSE for data when fibre size is not taken into account.

a/R	RMSE Cu			RMSE Mg		
	Torquato	Czapla	C-M	Torquato	Czapla	C-M
0.04	0.0059	0.0055	0.0254	0.0351	0.0919	0.1817
0.06	0.0054	0.0087	0.0303	0.0603	0.1207	0.2110
0.08	0.0084	0.0117	0.0323	0.0734	0.1343	0.2242
0.10	0.0168	0.0212	0.0426	0.18021	0.2421	0.3311
all	0.0102	0.0131	0.0332	0.1033	0.1579	0.2436

Table 2 presents the dimensionless effective thermal conductivity and coordination number and their respective standard deviations averaged over all fibre sizes as a function of fibre volume fraction. In the case of the ETC standard deviation ($\sigma(k/k_0)$) increases with the fibre volume fraction for both high and low conductivity ratio (k_1/k_2). It means that data are more dispersed for higher volume fraction and it can be observed in Fig. 4. Remarkably, the standard deviations for CNs (Tab. 2, $\sigma(Z_4)$) decrease with increasing mean CN (and increasing volume fraction) so CNs dispersion lowers. Although, for high conductivity ratio standard deviations for

the mean effective thermal conductivity data (Tab. 2) are few times higher than for low conductivity.

Table 2: Mean values (fibre size averaged) of the dimensionless effective thermal conductivity, and coordination number with their respective standard deviations for different fibre volume fractions.

f	$\overline{\frac{k}{k_0}}$ (Cu)	$\sigma(\overline{\frac{k}{k_0}})$	$\overline{\frac{k}{k_0}}$ (Mg)	$\sigma(\overline{\frac{k}{k_0}})$	$\overline{Z_4}$	$\sigma(Z_4)$
0.30	1.52980	0.007	1.9605	0.0298	1.9260	0.1624
0.40	1.77870	0.011	2.5669	0.0710	2.8210	0.1380
0.49	2.05368	0.018	3.3967	0.1425	3.7347	0.1154

Qualitatively results in Tab. 2 are in agreement with the data in Fig. 4 and Tab. 1 – discrepancy between numerical data and obtained from the analytical formulae increases for higher fibre volume fraction (f), dimensionless fibre size (a/R) and fibre/matrix thermal conductivity ratio (k_1/k_0).

7.1 Correlation for ETC

Equations (4) and (17) were used to correlate the coordination number Z_4 with the parameter ζ_2. Eliminating the fibre volume fraction between two formulae and truncating the result to the quadratic term the following relation for the infinite isotropic two-dimensional composite with random distribution of unidirectional fibres according to the RSA pattern:

$$\zeta_2\left(Z_4\right) = -0.0046\ {Z_4}^{\,2} + 0.0579\ Z_4\ . \tag{26}$$

To take into account the finite size of the composite, a correlation parameter CF was introduced

$$\widetilde{\zeta_2} = CF\,\zeta_2\ . \tag{27}$$

Values obtained from Eq. (3) with $\widetilde{\zeta_2}$ replacing of ζ_2 were fitted to numerical data to obtain the CF parameter. In the limiting case of the infinite medium ($a/R = 0.0$), the CF parameter tends to unity and the proposed formula for the ETC should be equivalent to Torquato's formula. The parameter CF was used to obtain a relation between Z_4 and $\widetilde{\zeta_2}$. A simple quadratic polynomial was used as the fitting curve

$$\widetilde{\zeta_2} = A\ {Z_4}^{\,2} + B\ Z_4\ . \tag{28}$$

The new parameters A and B depend on the dimensionless fibre size (a/R) and the contrast parameter β defined in Eq.(2). Therefore, at first the quadratic relation between A and B and (a/R) was assumed:

$$A = C\left(\frac{a}{R}\right)^2 + D\left(\frac{a}{R}\right) + E\,, \tag{29}$$

$$B = F\left(\frac{a}{R}\right)^2 + G\left(\frac{a}{R}\right) + H\,, \tag{30}$$

where $E = -0.0046$, $H = 0.0579$. Then linear dependence the parameters C, D, F, G on β was proposed, i.e.,

$$y = I\ \beta + J\,, \tag{31}$$

where the symbol y stands for C, D, F, G and I, J are constants given in Tab. 3.

Table 3: Correlation constants for Eq. (31).

Y	C	D	F	G
I	0.2461	-0.0723	-2.8127	0.8823
J	-0.6632	0.0782	8.0196	-0.9561

Equations (28)–(30) and (31) both with data given in Tab. 3 forms relations which could be used with Eq. (3) for prediction of the effective thermal conductivity of the finite size composite with random distribution of the unidirectional aligned fibres obtained with RSA sampling method inside circular matrix. In the case of $a/R = 0$, the following relation holds $A{=}E$, $B{=}H$ and Eq. (28) reduces to Eq. (26).

The dimensionless ETC, as a function of the fibre volume fraction, calculated from Eqs. (28)–(31) and the relation (17) are plotted in Fig. 5. In the case of low conductivity ratio (Fig. 5a) all curves practically merge. For high conductivity ratio and high-volume fractions (Fig. 5b) curves significantly diverge. In general, with increasing fibre volume fraction data becomes more dispersed and precision of the correlation lowers. The respective RMSE for obtained correlation and numerical data are summarized in Tab. 4 (a).

The effective thermal conductivity values obtained from numerical treatment and the proposed correlation, given by Eqs. (28)–(31) with formula for

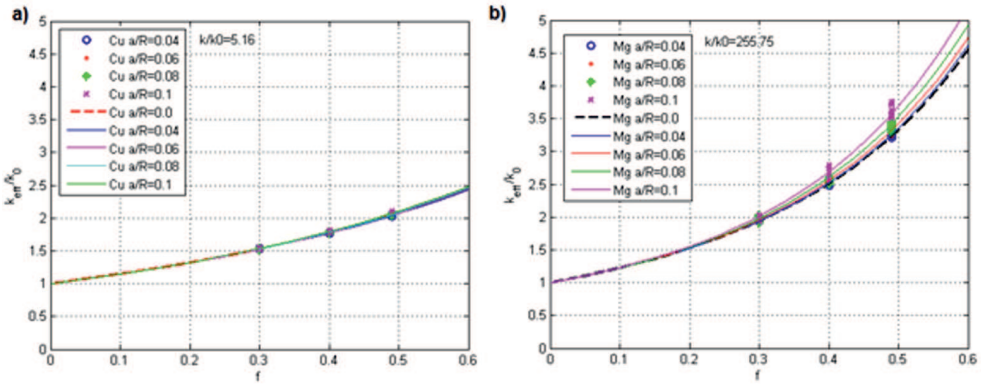

Figure 5: Effective thermal conductivity as a function of fibre volume fraction: a) for Cu; and b) for Mg matrix. Results given by solid and dashed lines were obtained by modified parameter Eqs. (28)–(31) with CN given by Eq. (17) and the effective conductivity Eq. (3). Graphical symbols correspond to numerical data. RMSE for curves is presented in Tab. 4 (a).

Table 4: Root mean squared error (RMSE) for ETC obtained from numerical simulation and calculated from correlation given by Eqs. (28)–(31). RMSE as a function of: a) fibre volume fraction f with CN given by Eq. (17) (corresponds to Fig. 5); b) Z_4 with application of Eq. (17) (Fig. 6); c) applying Z_4 calculated by sequential analysis for every single geometry pattern.

a/R	RMSE (a)		RMSE (b)		RMSE (c)	
	Cu	Mg	Cu	Mg	Cu	Mg
0.04	0.0053	0.0260	0.0491	0.0553	0.0054	0.0269
0.06	0.0051	0.0281	0.0733	0.0783	0.0053	0.0296
0.08	0.0080	0.0447	0.1180	0.1260	0.0078	0.0451
0.10	0.0098	0.0574	0.1421	0.1530	0.0103	0.0631

the CN given by Eq. (17) is plotted in Fig. 6. Dispersion between the data increases with the fibre/matrix thermal conductivity ratio, particle size and fibre volume fraction. The obtained correlation using the CN seems to be less accurate than directly using the fibre volume fraction (Fig. 5) as indicated in Tab. 4 (b). Applying coordination numbers computed separately for every geometrical pattern (not from Eq. (17)) and putting them into the proposed correlation given by Eqs. (28)–(31) leads to better agreement – see Tab. 4 (c).

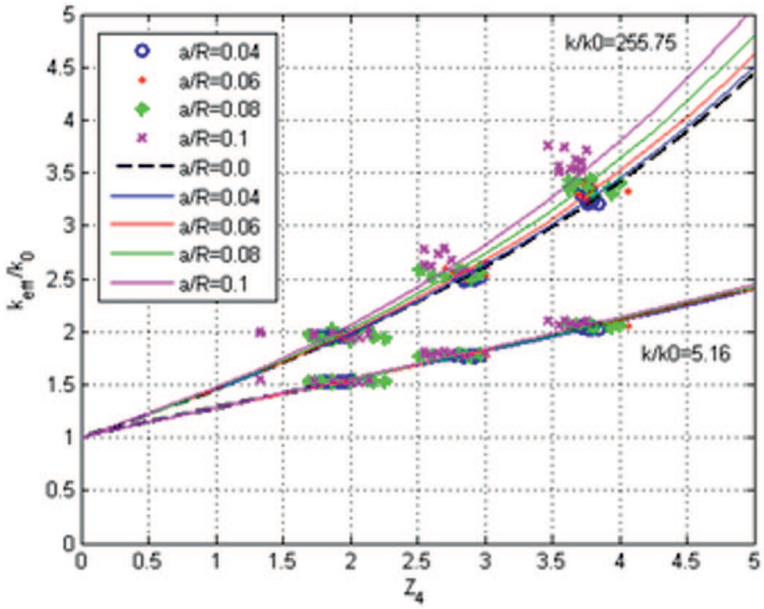

Figure 6: Effective thermal conductivity *vs.* coordination number given by Eq. (3) with ζ_2 given by Eqs. (28)–(31) and coordination number given by correlation Eq. (17). RMSE for those curves is presented in Tab. 4 (b). Graphical symbols correspond to numerical data.

7.2 Anisotropy and symmetry of the effective thermal conductivity tensor

In order to investigate symmetry of conductivity tensor (see Eq. (19)) components k_{yx}, k_{xx} and k_{xy}, k_{yy} were calculated numerically using Eqs. (A19)–(A21), and (A22) for two extreme cases $f = 0.49$ with $a = 0.04R$ and $f = 0.3$ with $a = 0.1R$ and only for high conductivity ratio case ($k_1/k_0 = 255.75$). Components k_{yx}, k_{xx} were calculated applying temperature gradient in X-direction only and similarly k_{xy}, k_{yy} were computed for temperature gradient in Y-direction only. Resulting conductivity tensor $\mathbf{K}$ was divided into symmetric ($\mathbf{K^s}$) and antisymmetric ($\mathbf{K^a}$) part, diagonalized (Eq. 23) and finally $\mathbf{\Lambda}$ was obtained, as described in Sec. 5. Finally, the principal components for the symmetric and antisymmetric parts of $\mathbf{\Lambda}$ tensor were obtained: k_{21}, k_{11} and k_{12}, k_{22}.

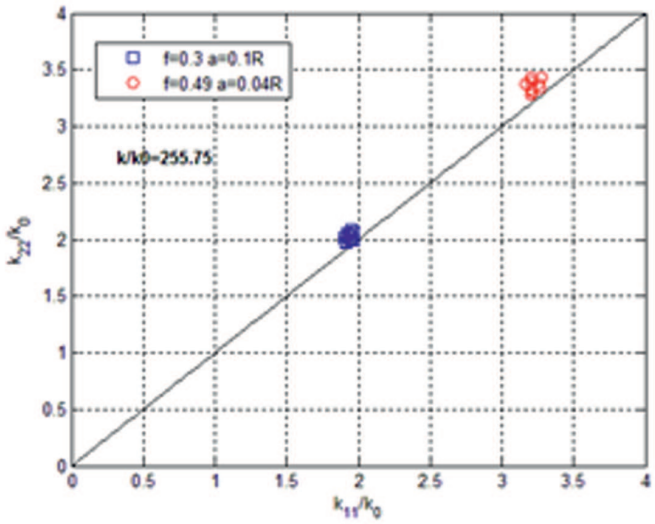

Figure 7: Comparison of conductivity tensor $\mathbf{\Lambda}$ diagonal components of the composite in the principal directions.

Figure 7 compares diagonal components of the effective thermal conductivity tensor $\mathbf{\Lambda}$ in principal frame of reference (Eq. 22), while Fig. 8 shows non-diagonal (unphysical) components of $\mathbf{\Lambda}$ tensor related to corresponding diagonal components (a) and matrix conductivity (b).

The root mean squared error (RMSE) was used as quantitative indicator of deviation of numerical data from transverse isotropy. The first case has $f = 0.3$ and $a = 0.1R$ and for diagonal elements it has RMSE $= 0.0658$, maximal relative difference between k_{11} and k_{22} was 7.09% (Fig. 7). For non-diagonal components RMSE=0.0220 and non-diagonals are less than 3% of corresponding diagonals (Fig. 8a). Maximum non-diagonal is less than 5% of matrix conductivity (Fig. 8b).

In case of high volume fraction ($f = 0.49$) and small particles ($a = 0.04R$) diagonal elements RMSE $= 0.1041$ (Fig. 8a). Maximum relative difference between k_{11} and k_{22} was 6.92%. For non-diagonal components RMSE $= 0.0166$ (Fig. 8a). Non-diagonal elements were less than 2% of diagonals (Fig. 8a) and maximum value was about 6% of matrix conductivity value. Some of the non-diagonal components of conductivity tensors were negative (Fig. 8), however all matrices as required were positively-definite [1].

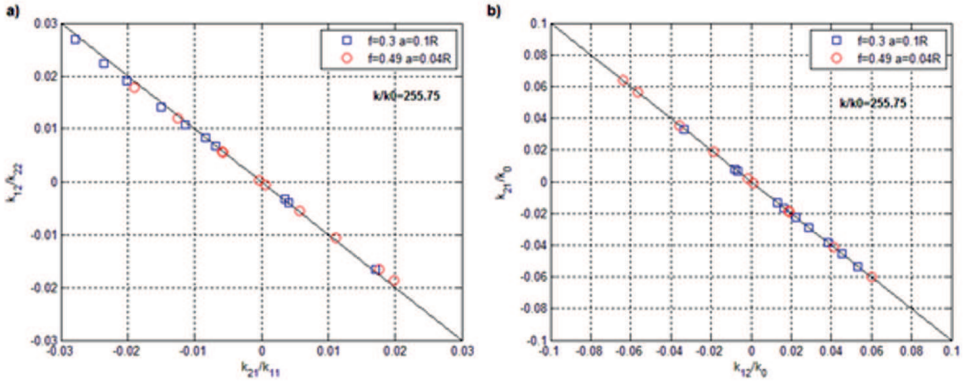

Figure 8: Comparison of non-diagonal components of conductivity tensor for principal directions of the composite: a) values relative to corresponding diagonal element of Λ tensor; b) values relative to matrix thermal conductivity

8 Conclusions

Numerical simulations were carried out in order to determine the effective thermal conductivity (ETC) of composites reinforced with unidirectional aligned fibres of circular cross-section. The fibres were randomly distributed in the matrix with the random geometry generated according to the RSA pattern. The finite domain of the composite was considered in the form a circle with a radius R. The way of determination of the effective thermal conductivity for this shape of the domain and transverse direction to fibre alignment was presented. The obtained ETC data were ensemble averaged and correlated with fibre/matrix thermal conductivity ratio and directly or indirectly (via the coordination number CN) with the volume fraction of fibres. The results were compared with analytical formulae proposed by Torquato and Lado – Eq. (3) and Czapla [13] for random and statistically isotropic distribution of fibres and infinite domain of the composite. Additionally, comparison was carried out with the well-known Claussius-Mossotti formula (Eq.(1)) valid for low volume fraction of fibres and not including mutual interaction of neighbour fibres. In all cases, as anticipated, the ETC calculated with Eq. (1) under predicted the numerical results. It was found that for small fibre/matrix thermal conductivity ratio k_1/k_0 the numerical simulations lead to values very close to these calculated from Torquato, Eq. (3) and Czapla, Eq. (5), formulae except for high values of fibre / composite radii ratio (a/R). For high k_1/k_0 values Czapla results

are significantly different than numerical. The results show that for small particles size, i.e., small values of a/R ratio, the numerical data are in good agreement with Eq. (3) but with increasing size of particles and increasing volume fraction, differences become remarkable. In order to treat the ETC as property of the composite its value should be independent of the shape and dimensions of the material. Therefore, the obtained results allow to evaluate what dimensions should the specimen have, e.g., in experiments, in order to determine its effective thermal conductivity as the bulk property.

The numerically calculated ETC for random composite was also correlated directly with the mean coordination number, i.e., the mean number of nearest neighbours to the selected fibre – see Fig. 6. Here it was found that for small values of a/R ratio the correlation is in good agreement with numerical data but with increasing size of particles and increasing volume fraction, the correlation seems to be worse. Therefore, it can be concluded that, the relation between the ETC and the volume fraction of fibres (f_1) seems less sensitive to volume fraction (f) than between the ETC and the mean coordination number to Z_4.

The problem of isotropy of the effective thermal conductivity tensor were investigated for two extreme cases: $f = 0.49$, $a = 0.04R$ and $f = 0.03$, $a = 0.1R$. Relatively high difference between components in principal directions (k_{11} and k_{22}) were observed reaching as high as 7% (Fig. 7). It leads to the conclusion of some level of anisotropy in fibre distribution for analysed geometries in XY-plane, i.e., transverse direction to fibres.

The effective thermal conductivity tensor should be symmetric, i.e., its non-diagonal elements should be zero in the principal frame of reference ($k^a_{12} = -k^a_{21} = 0$ in Eq. (23)). In calculations presented here this condition was satisfied within 3% accuracy in relation to the diagonal elements (Fig. 8a). Possible reason are numerical errors or errors introduced by applied methods.

Summing up, relatively simple correlations (Eqs. (28)–(31), Tab. 3), to apply with Eq. (3), were proposed. They can be used to estimate influence of existence of composite boundaries on the effective thermal conductivity of the composite material. Those correlations are equivalent with Torquatos correlation (Eq. (3)) in the case of very small fibres in comparison to size of the composite matrix. The use of the correlation between the coordination number and conductivity is an alternative to the application of the correlation between conductivity and volume fraction.

Acknowledgements This work has been supported by the the Polish National Centre for Research and Development within European Regional Development Fund under the Operational Program Innovative Economy No POIG.01.01.02-00-097/09 'TERMET – New structural materials with enhanced thermal conductivity'.

Received 6 July, 2017

References

[1] Torquato S.: *Random Heterogeneous Materials – Microstructure and Macroscopic Proporties* (S. Antman, Ed.), Springer-Verlag, 2002.

[2] Schreiner W. and Kratky K.W.: *Computer simulation of hard-disk packings with spherical boundary conditions.* J. Chem. Soc. Faraday Trans. **2**(1982), 78, 379–389.

[3] Antwerpen W.V.:, Toit C.D, Rousseau P.: *A review of correlations to model the packing structure and effective thermal conductivity in packed beds of mono-sized spherical particles.* Nucl. Eng. Des. **240**(2010), 10, 1803–1818.

[4] Pietrak K.and Wiśniewski T.S.: *A review of models for effective thermal conductivity of composite materials.* J. Power Technol. **1**(2015), 14–24.

[5] Torquato S., Uche O.U. and Stillinger F.H.: *Random sequential addition of hard spheres in high Euclidean dimensions.* Phys. Rev. E, **74**(2006), 061308-1–061308-16.

[6] Darnowski P., Furmański P., Domański R.: *Coordination number for random distribution of parallel fibres.* Arch. Thermodyn. **38**(2017), 1, 3–26.

[7] Jouannot-Chesney P., Jernot J. and Lantuejoul C.: *Practical determination of the coordination number in granular media.* Image Anal. Stereol **25**(2006), 55–61.

[8] Huerta A., Naumis G.G.: *Role of rigidity in the fluid-solid transition.* Phys. Rev. Lett. **90**(2003), 14, 145701-1–14570-4.

[9] Largo J., Solana J.: *Theory and computer simulation of the coordination number of square-well fluids of variable width.* Fluid Phase Equilibr. **193**(2002), 1-2, 277–287.

[10] Rayleigh L.: *On the influence of obstacles arranged in a rectagular order upon the proporties of medium.* Phil. Mag. **34**(1892) 481–502.

[11] Czapla R., Nawalaniec W., Mityushev V.: *Effective conductivity of random two-dimensional composites with circular non-overlaping inclusions.* Comp. Mater, Sci. **63**(2012), 118–126.

[12] Fiedle T., Pesetskay E., Ochsne A., Gracio J.: *Calculations of the thermal conductivity of porous media.* Materials Science Forum, DOI:10.4028/www.scientific.net/MSF.514-516.754, 514:754–758, 01/2006.

[13] Torquato S.: *Effective electrical conductivity of two-phase disordered composite media.* J Appl. Phys. **58**(1985), 10, 3790–3797.

[14] Torquato S., Lado F., Fisher M.E.: *Bounds on the conductivity of a random array of cylinders*. Proc. Royal Soc. Lond. A, **417**(1988), 1852, 59–80.

[15] Furmański P.: *Heat conduction in composites: Homogenization and macroscopic behavior*. Appl. Mech. Rev. **50**(1997), 6, 327–356.

[16] Perrins W.T., McKenzie D.R., McPhedran R.: *Transport proporties of regular arrays of cylinders*. Proc. R. Soc. Lond. A, **369**(1979), 1737, 207-225.

[17] Hinrichsen E.L., Feder J., Jossang T.: *Geometry of random sequential adsorption*. J. Stat. Phys. **44**(1986), 5/6, 793–827.

[18] Farlow S.J.: *Partial Differential Equations for Scientist and Engineers*. Dover Pub. 1993.

[19] Liu S., Zhang Y.: *Multi-scale analysis method for thermal conductivity of porous material with radiation*. Multidiscipline Model. Mater. Struct., Emerald, **2**(2012), 3, 327–344.

[20] Furmański P., Gogół W.: *Fundamentals of heat conduction in anisotropic media*. Bull. Inst. Heat Eng. **46**(1977).

[21] Chen Q., Wang M., Guo Z., Pan N.: *Irreversibility of heat conduction in the complex multiphase systems and its application to the effective thermal conductivity of porous media*. Int. J. Nonlin. Sci. Num. **10**(2009), 1, 7–16.

[22] Wang M., Pan N.: *Modeling and prediction of the effective thermal conductivity of random open-cell porous foams*. Int. J. Heat Mass Tran. **51**(2008), 5-6, 1325–1331.

[23] *ANSYS FLUENT 13.0.0 User's Guide*, 2010.

[24] *Gambit 2.4 User's Guide*, 2007.

[25] McQuarrie D.A.: *Mathematical Methods for Scientists and Engineers*. University Science Books Suasalito 2003.

[26] Smith P.A., Torquato S.: *Computer simulation results for bounds on the effective conductivity of composite nedia*. J. Appl. Phys. **65**(1989), 3, 893–900.

[27] Jopek H., Strek H.T.: *Optimization of the effective thermal conductivity of a composite*. In: Convection and Conduction Heat Transfer, (A. Ahsan, Ed.), InTech, Rijecka 2011, 197–214.

[28] Glandt E.D.: *Continuity between disorder and order in the sequential deposition of particles*. Chem. Eng. Commun. **19**(2005), 2, 1405–1423.

[29] Material Property MatWeb: *Proporties of diamond, copper and magnesium* 11 2012, www.matweb.com.

[30] Kidalov S.V., Shakhov F.M.: *Thermal conductivity of diamond composites*. Materials **2**(2009), 2467–2495.

[31] Shinde S.L., Goela J.S.: *High Thermal Conductivity Materials*. Springer, 2006.

APPENDIX

A. Derivation of expressions for calculation of components of the effective thermal conductivity tensor

The effective thermal conductivity for heterogeneous media and slowly varying, in space and time, temperature distribution is given by the relation similar to the Fourier law [1,18,19]:

$$\langle \vec{q} \rangle = -\mathbf{K} \cdot \langle \nabla T \rangle \ , \tag{A1}$$

where $\langle \vec{q} \rangle$ is the mean heat flux vector, $\langle \nabla T \rangle$ is the mean temperature gradient and $\mathbf{K}$ is 3 x 3 thermal conductivity tensor and $\langle\rangle$ denotes volume averaging procedure [19,20]

$$\langle w \rangle = \frac{1}{V} \int_V w dV \ . \tag{A2}$$

The analysis starts with $\vec{q} \otimes \vec{r}$ outer product of the vectors $\vec{q}$ and $\vec{r}$. Generalized chain rule allows to transform divergence of this product into the form

$$\nabla \cdot (\vec{r} \otimes \vec{q}) = (\nabla \otimes \vec{r}) \cdot \vec{q} + \vec{r}(\nabla \cdot \vec{q}) \ . \tag{A3}$$

Outer product of the nabla operator and the location vector is the unit tensor $\nabla \otimes \vec{r} = \mathbf{I}$, so

$$\nabla \cdot (\vec{r} \otimes \vec{q}) = \vec{r}(\nabla \cdot \vec{q}) + \vec{q} \, . \tag{A4}$$

In order to eliminate $\nabla \cdot \vec{q}$ the energy equation without heat sources was introduced [25]

$$\rho c_p \frac{\partial T}{\partial t} + \nabla \cdot \vec{q} = 0 \tag{A5}$$

and by combining Eqs. (A4) and (A5) relation for the heat flux is given by

$$\vec{q} = \nabla \cdot (\vec{r} \otimes \vec{q}) + \vec{r} \left(\rho c_p \frac{\partial T}{\partial t} \right) \ . \tag{A6}$$

Volume averaging of both sides of the latter expression and application of the relation (A1) leads to the formula

$$\left\langle \nabla \cdot (\vec{r} \otimes \vec{q}) + \vec{r} \left(\rho c_p \frac{\partial T}{\partial t} \right) \right\rangle = -\mathbf{K} \cdot \langle \nabla T \rangle \ , \tag{A7}$$

which can be transformed to

$$\frac{1}{V}\int_V \nabla\cdot(\vec{r}\otimes\vec{q})\,dV+\frac{1}{V}\int_V \vec{r}\left(\rho c_p\frac{\partial T}{\partial t}\right)dV=-\mathbf{K}\cdot\langle\nabla T\rangle\ . \tag{A8}$$

It is convenient to introduce generalized divergence theorem to replace volumetric integral with surface integral [1]

$$\oint_A(\vec{r}\otimes\vec{q})\cdot\vec{n}dA+\int_V \vec{r}\left(\rho c_p\frac{\partial T}{\partial t}\right)dV=-\mathbf{K}\cdot\langle\nabla T\rangle\ . \tag{A9}$$

The integrand in the first term on the left hand side of Eq. (A9), taking into account fact that $\vec{r}=\left[\begin{array}{ccc} x & y & z\end{array}\right]^T$, $\vec{q}=\left[\begin{array}{ccc} q_x & q_y & q_z\end{array}\right]^T$ and $\vec{n}=\left[\begin{array}{ccc} n_x & n_y & n_z\end{array}\right]^T$, can be expressed as

$$(\vec{r}\otimes\vec{q})\cdot\vec{n}=\left[\begin{array}{ccc} xq_x & xq_y & xq_z\\ yq_x & yq_y & yq_z\\ zq_x & zq_y & zq_z\end{array}\right]\cdot\left[\begin{array}{c} n_x\\ n_y\\ n_z\end{array}\right]=$$

$$=\left[\begin{array}{ccc} n_xq_xx+ & n_yq_yx+ & n_zq_zx\\ n_xq_xy+ & n_yq_yy+ & n_zq_zy\\ n_xq_xz+ & n_yq_yz+ & n_zq_zz\end{array}\right]=\left[\begin{array}{c} x(\vec{q}\cdot\vec{n})\\ y(\vec{q}\cdot\vec{n})\\ z(\vec{q}\cdot\vec{n})\end{array}\right]\ . \tag{A10}$$

If temperature gradient is only applied in Y-direction then

$$\langle\nabla T\rangle=\left[\begin{array}{ccc} 0 & \left\langle\frac{\partial T}{\partial y}\right\rangle & 0\end{array}\right]^T. \tag{A11}$$

For the assumed constant value of the mean temperature gradient and the steady state of heat conduction

$$\left\langle\frac{\partial T}{\partial y}\right\rangle=\text{const}\ . \tag{A12}$$

$$\frac{\partial T}{\partial t}=0\ . \tag{A13}$$

Finally, taking into account Eqs. (A9)–(A11), (A13) and Eq. (19) the general equation combining heat flux with conductivity can be written as

$$\oint_A\left[\begin{array}{c} x(\vec{q}\cdot\vec{n})\\ y(\vec{q}\cdot\vec{n})\\ z(\vec{q}\cdot\vec{n})\end{array}\right]dA=\ =-\mathrm{V}\left[\begin{array}{ccc} \mathrm{k_{xx}} & k_{xy} & 0\\ k_{yx} & \mathrm{k_{yy}} & 0\\ 0 & 0 & \mathrm{k_{zz}}\end{array}\right]\cdot\left[\begin{array}{c} 0\\ \left\langle\frac{\partial T}{\partial y}\right\rangle\\ 0\end{array}\right]\ . \tag{A14}$$

Therefore, according to Eq. (A1):

$$\langle q_y \rangle = \frac{1}{V} \oint_A (\vec{q} \cdot \vec{n}) y dA = -k_{yy} \cdot \left\langle \frac{\partial T}{\partial y} \right\rangle , \tag{A15}$$

$$\langle q_x \rangle = \frac{1}{V} \oint_A (\vec{q} \cdot \vec{n}) x dA = -k_{yx} \cdot \left\langle \frac{\partial T}{\partial y} \right\rangle , \tag{A16}$$

and hence

$$k_{yy} = \frac{-\oint_A y(\vec{q} \cdot \vec{n}) dA}{\left\langle \frac{\partial T}{\partial y} \right\rangle \cdot V} , \tag{A17}$$

$$k_{xy} = \frac{-\oint_A x(\vec{q} \cdot \vec{n}) dA}{\left\langle \frac{\partial T}{\partial y} \right\rangle \cdot V} . \tag{A18}$$

In the similar manner, it is possible to obtain the ETC components when the

$$k_{xx} = \frac{-\oint_A x(\vec{q} \cdot \vec{n}) dA}{\left\langle \frac{\partial T}{\partial x} \right\rangle \cdot V} , \tag{A19}$$

$$k_{yx} = \frac{-\oint_A y(\vec{q} \cdot \vec{n}) dA}{\left\langle \frac{\partial T}{\partial x} \right\rangle \cdot V} . \tag{A20}$$

B. Examples of temperature distributions in the composite reinforced with randomly dispersed unidirectional fibres

Some example temperature distribution in the composite for random distribution of fibres and based on numerical calculations are shown below

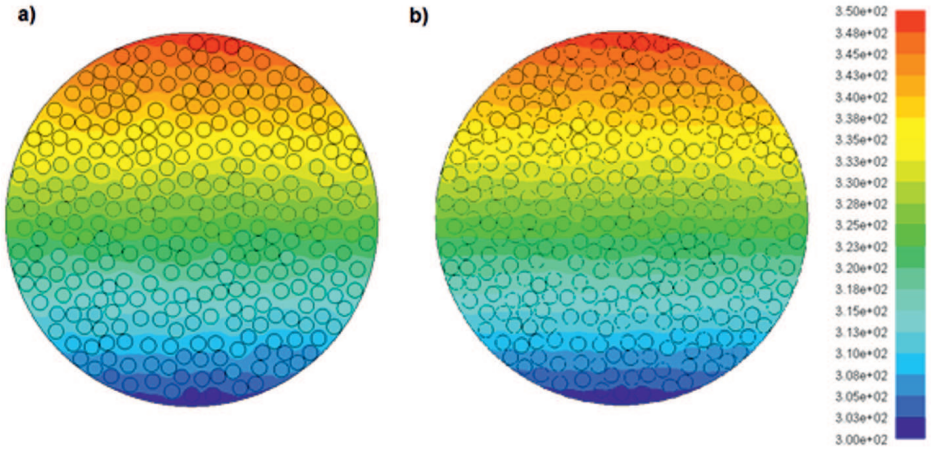

Figure B1. Temperature distribution in composites with r/R=0.04, f=0.49 and 306 particles for: a) k_1/k_0=255.75, $\frac{k_{eff}}{k_0}$=3.23; b) for $\frac{k_1}{k_0}$=5.16, $\frac{k_{eff}}{k_0}$=2.03.

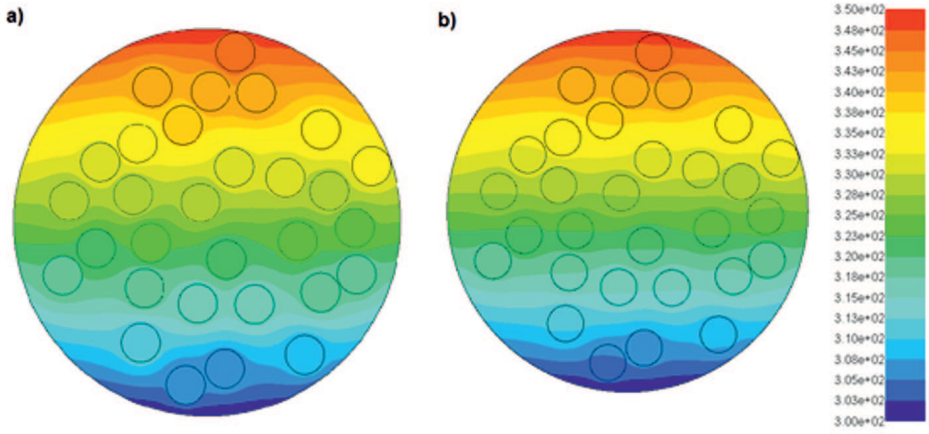

Figure B2. Temperature distribution in composites with r/R=0.1, f=0.3 and 30 particles for: a) k_1/k_0=255.75, $\frac{k_{eff}}{k_0}$=2.00; b) for $\frac{k_1}{k_0}$=5.16, $\frac{k_{eff}}{k_0}$=1.54.